CHALMERS
UNIVERSITY OF TECHNOLOGY

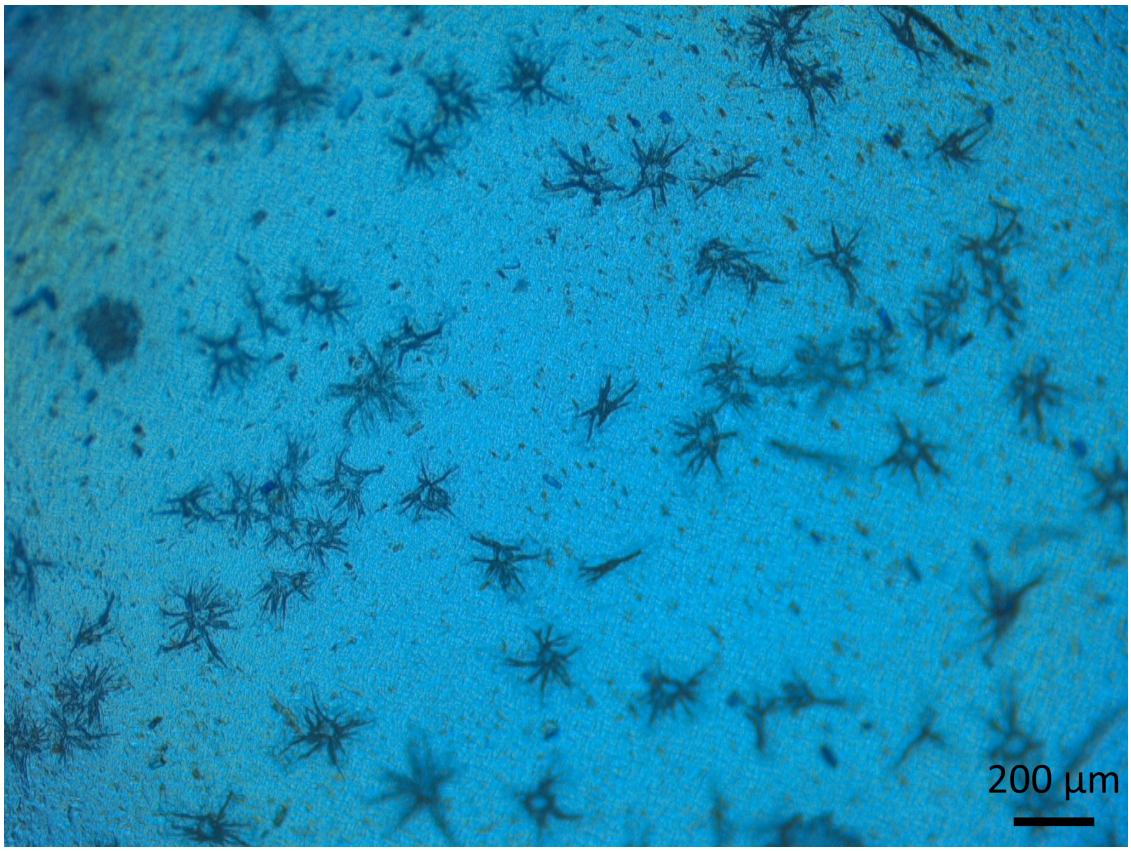

Transparent conducting water stable films of cellulose nanocrystals

Master Degree Report in Programme Materials Chemistry

YUGE YAO

DEPARTMENT OF CHEMISTRY AND CHEMICAL ENGINEERING
CHALMERS UNIVERSITY OF TECHNOLOGY
Gothenburg, Sweden 2024
www.chalmers.se

Degree project report 2024

Transparent conducting water stable films of cellulose nanocrystals

YUGE YAO

CHALMERS

Department of Chemistry and Chemical Engineering
Chalmers University of Technology
Gothenburg, Sweden 2024

Transparent conducting water stable films of cellulose nanocrystals
Yuge Yao

Supervisor: Jelka Feldhusen, Department of Chemistry and Chemical Engineering
Examiner: Gunnar Westman, Department of Chemistry and Chemical Engineering

Degree project report 2024
Department of Some Subject or Technology
Chalmers University of Technology
SE-412 96 Gothenburg
Sweden
Telephone +46 0724436897

Polarized Optical Microscopy picture of the water-stable films of cellulose nanocrystals

Gothenburg, Sweden 2024

Transparent conducting water stable films of cellulose nanocrystals
Yuge Yao
Department of Chemistry and Chemical Engineering.
Chalmers University of Technology

Abstract

Abstract: Sulfated cellulose nanocrystals (CNC), a promising renewable biopolymer, have been utilized as templates along with conductive organic polymers (COPs) to prepare flexible, transparent, water-stable conductive films for optoelectronic applications. Triethanolamine (TEOA), sodium hypophosphite (SHP), 1,2,3,4-butanetetracarboxylic acid (BTCA), and ethylene glycol diglycidyl ether (EGDE) were chosen as crosslinkers, and a flexible, water-stable, transparent CNC film was successfully prepared. Two approaches, in-situ and ex-situ methods, were then employed for preparing the transparent conductive films. The lowest sheet resistance of the CNC/Pyrrole film was 2.2×10^8 ohm/sq using the ex-situ fabrication method. Characterization techniques including titration, polarized optical microscopy, ATR-FTIR spectroscopy, and sheet resistance measurement were employed to analyze and observe the films. The challenges faced during using both methods are also discussed.

Keywords: Conductive, Water resistant, Transparent, Cellulose nanocrystal films

Acknowledgements

I appreciate Gunnar for introducing me to the group and providing me with various learning resources. The most valuable lesson I learned from this project is that when solving a problem, the procedure is to promptly act on an idea, engage in trial and error, analyze and understand the reasons behind the outcomes, leading to the generation of new ideas, and then repeat this loop.
A lot of thanks to my good friends all along the way. I couldn't express how much I am supported and inspired by your kindness and wisdom.

"合抱之木，生于毫末" For each towering giant of a tree, a tiny bud it used to be. Thanks for the rain and shine, I'm gradually growing like a tree through the ages.

Yuge Yao, Gothenburg, April 2024

List of Acronyms

Below is the list of acronyms that have been used throughout this thesis listed in alphabetical order:

CNC	Cellulose Nanocrystal
CNF	Cellulose Nanofibers
BNC	Bacterial Nanocellulose
SCNC	Sulfated Cellulose Nanocrystals
ATR-FTIR	Attenuated Total Reflection Fourier Transform Infrared
MS	Mass Spectrometry
TEOA	Triethanolamine
NNNN	N,N,N',N',-Tetramethyl-1,4-diaminobutane
EGDE	Ethylene glycol diglycidyl ether
SHP	Sodium hypophosphite
EDOT	3,4-Ethylenedioxythiophene
BTCA	1,2,3,4-Butanetetra-carboxylic acid
PPS	Potassium persulfate
PSS	Poly(styrenesulfonic acid)
PEDOT	Poly(3,4-ethylene dioxythiophene)
PANI	Polyaniline
PLED	Polymeric Light-Emitting Diodes
NMR	Nuclear Magnetic Resonance
OLED	Organic Light-Emitting Diodes
SMU	Source Measurement Unit
4PP	Four Point Probe
Rs	Sheet resistance

Contents

List of Figures

List of Tables

1
Introduction

1.1 Background

The energy crisis and environmental problems caused by hazardous recalcitrant compounds from petroleum hydrocarbon pollutants have drawn attention to lignocellulose biopolymers as potential solutions. Among the main components of lignocellulose, namely cellulose, hemicellulose, and lignin, cellulose stands out as the most abundant natural renewable biopolymer [7]. Cellulose, with the chemical formula $(C_6H_{10}O_5)_n$, is a carbohydrate linear polymer composed of repeated β-D-glucopyranose units linked by β $(1 \rightarrow 4)$ bonds, with three hydroxyl groups per anhydroglucose unit, providing a high capacity for surface modification [29]. While cellulose is naturally present in plants as a biocomposite, it can also be extracted from other natural sources, including bacteria, algae, and sea animals. Cellulose, as an emerging renewable nanomaterial, finds various applications in food, paper production, industrial, and pharmaceutical biomaterials [3] [16]. Nano-cellulose is classified into three main categories based on sources and morphological structures: cellulose nanocrystals (CNC), cellulose nanofibers (CNF), and bacterial nanocellulose (BNC) [28].

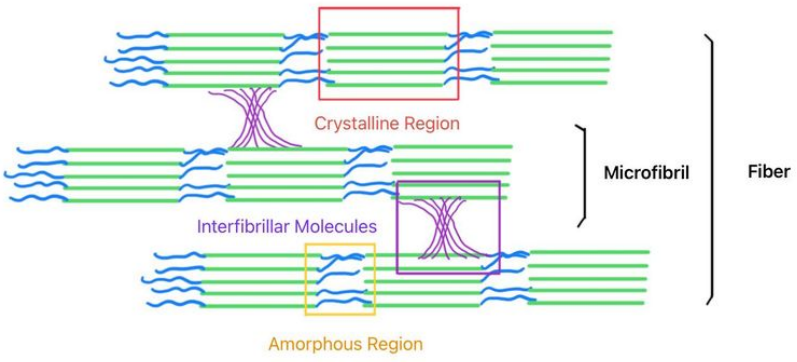

Figure 1.1: Scheme of cellulose nanofibers (CNF)

CNC is currently considered the most practical nanocellulose for various applications due to its ability to be manufactured on an industrial scale. Industrial CNC products are obtained after fractionation and pre-treatment processes. Typically, fractionation involves removing hemicellulose and lignin. Following fractionation,

nanocellulose can be extracted from the pretreated cellulosic materials through mechanical treatment, acid hydrolysis, enzymatic hydrolysis, or a combination of these processes.

An acid-induced destructuring process using hydrochloric, hydrobromic, or sulfuric acids is commonly employed to isolate CNC. During acid hydrolysis, acid molecules selectively permeate the amorphous (disordered) cellulose fiber domains and break glycoside bonds, yielding CNC and sugar molecules. Consequently, CNC is extracted from the relatively resistant crystalline (ordered) regions of cellulose. The most common extraction method involves sulfuric acid, where the sulfuric acid introduces half-ester sulfate groups via reaction with hydroxyl groups on the cellulose surface, resulting in CNC with excellent aqueous stability. [23]

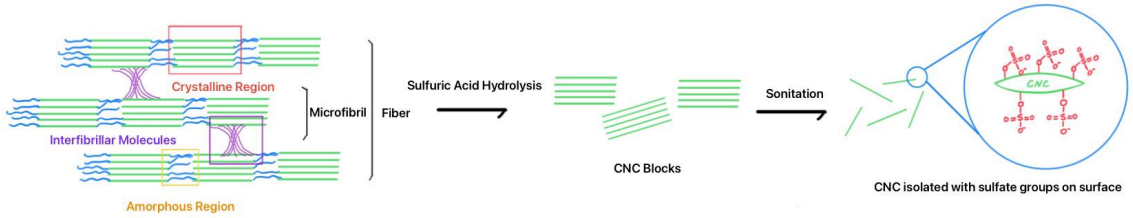

Figure 1.2: Scheme of sulfated cellulose nanocrystals (CNC) prepared from CNF

Due to the fascinating properties exhibited by CNC, such as biodegradability, nontoxicity, hydrophilicity, and the ability to self-assemble in liquid states, it has found extensive use as an emulsifier, thickener, and stabilizer in cosmetics, and pharmaceutical applications. Besides, in heavy-duty engineering applications, CNC's low density, remarkable mechanical properties, and nanoscale dimensions, which afford high surface areas, make them ideal candidates as fillers or reinforcement agents. This utilization is prevalent in industries such as automobile, aerospace, and certain biomedical fields, facilitating the production of high-performance materials. These materials benefit from the excellent thermal stability, superior mechanical strength, and optical properties offered by CNC nanoparticles.[11][28]

1.1.1 Sulfated Cellulose Nanocrystals

CNCs are highly crystalline and needle-shaped structured with typical dimensions of 4-20 nm in width and 100-500 nm in length that gives them a high aspect ratio of about 10-70. The geometrical dimension, biological, chemical, and mechanical properties of CNC depend on the pristine cellulosic material and its processing conditions.[23][1]
Cellulose nanocrystals prepared via sulfuric acid hydrolysis are decorated with sulfate groups that yield a stable water suspension. In this thesis, all CNC utilized were derived from cellulose hydrolyzed with sulfuric acid, resulting in charged nanocrystals wherein some surface hydroxyl (OH) groups have been replaced with $-OSO_3^-$ groups. The quantity of sulfate-substituted hydroxyl groups can be adjusted, thereby influencing their solubility and potential for functionalization. The

properties of the polysaccharides can be modified through chemical modifications of the sulfate groups on the cellulose.[17]

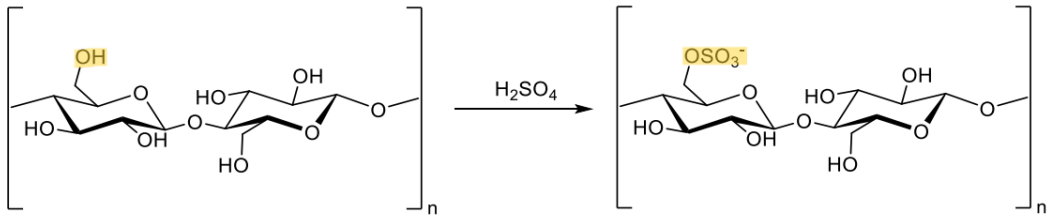

Figure 1.3: Scheme of surface hydroxyl groups on CNC be replaced by sulfate groups.[17]

Sulfated nanocellulose is highly hydrophilic, making it challenging to disperse and mix with hydrophobic matrices for producing cellulose-based composite materials. To enhance the chemical compatibility between CNCs and a matrix, or to further render the products hydrophobic, CNCs are typically hydrophobized either by adsorbing hydrophobic cations onto the sulfate groups or by chemically modifying the CNC surfaces. Films produced from sulfated-CNC disperse when placed in water due to weak forces between crystallites, allowing water to diffuse into the crystallite network and disperse them. To make the film water-resistant, a cross-linker is usually added to link the crystals. Short linkers may result in stiffness of the films, whereas longer linkers, consisting of 25 or more atoms, may cause the film to swell and turn into a gel. In this thesis, various types of crosslinkers and azetidinium salts (Az-salts) are explored to improve the CNC surface and produce the flexible, water-resistant CNC films.[6]

1.2 Cellulose Nanocrystals Films

CNC suspensions have the ability to self-organize into a liquid crystalline arrangement, which can be preserved when the suspensions are carefully dried. This self-organization can be observed through fingerprint patterns indicative of chiral-nematic ordering when the suspensions are visualized by polarized optical microscopy. The chiral nematic structures consist of stacked planes of CNCs aligned along a vector, with the orientation of each director rotated about the perpendicular axis from one plane to the next. This self-arrangement is sensitive to the surrounding environment, including factors such as viscosity, ionic strength, pH, external fields, and drying conditions. Therefore, preserving such organization in a polymer matrix poses a significant challenge.[21]

1.2.1 Transparency of CNC Films

CNC chiral nematic structure can be preserved after the controlled drying of suspensions that allows formation of iridescent films of CNCs with a chiral nematic pitch

on the same length scale as the visible light wavelength. This unique system was described as an interference device with a capacity to reflect circularly polarized light over a specific wavelength range. Thin solid films that retain CNC optical properties have numerous potential applications like coating for decorative materials, security papers, and so on. However, the critical point for the practical application of such films based on the pure CNCs is their hygroscopic character arising from the inherent hydrophilic nature of cellulose. Therefore, from a practical point of view, achieving and preserving this spectacular self-organization in a polymer matrix represents a challenge for application in coating decorative materials.[21] Properties of films derived from aqueous nanocrystals cellulose dispersions by water evaporation depend on concentration of sulfate groups.

1.3 Flexible Water-resistant CNC Films

As hydrophilic CNC is a rigid rod-shaped particle with high modulus, CNC films are very fragile. In order to overcome this limitation, Triethanolamine (TEOA) has been used to improve the flexibility of CNC liquid crystal films. Furthermore, the pure CNC films have strong water absorption ability and are highly soluble in water, resulting in rapid dissolution of the film in aqueous solutions. Meanwhile, water molecules enter the interior of CNC films, increasing the permeability of CNC. As a result, the CNC film disappears in water quickly, greatly limiting the application scope.[4]

TEOA has the potential to enhance the flexibility of sulfated cellulose nanocrystals (CNCs). Aggregation of CNCs can result in localized regions of increased stiffness or brittleness within the composite material. TEOA as a dispersant can help to prevent CNC aggregation both in solution and within the polymer matrix. By facilitating improved dispersion of CNCs, TEOA fosters a more uniform distribution and alignment of CNCs within the polymer matrix, thus leading to enhanced flexibility. Additionally, TEOA-modified CNCs may improve compatibility with the polymer matrix, further contributing to the overall flexibility of the composite material.

The Ethylene glycol diglycidyl ether (EGDE), 1,2,3,4-Butanetetra-carboxylic acid (BTCA), and Sodium hypophosphite (SHP) are discussed in this theis to enhance the water resistance of sulfated cellulose nanocrystals (CNCs) by serving as crosslinkers.

EGDE is a bifunctional epoxy compound that can react with hydroxyl groups present on the surface of CNCs. During crosslinking, EGDE molecules may form the covalent bonds with hydroxyl groups on adjacent CNCs, creating a network structure within the composite material. This crosslinked network helps to physically trap water molecules and prevent them from penetrating the CNC matrix. BTCA has been enhanced as an efficient crosslinker for the fabrication of freestanding crosslinked nanocellulose membranes. Evidence indicates that it not only improves the water stability of CNC membranes but also introduces a carboxyl group to the crosslinked material for every crosslink created between the cellulose and BTCA. Additionally,

it shows good ion transport properties.[37] SHP contains phosphorus atoms that can react with hydroxyl groups present on the surface of CNCs. When mixed with CNCs and heated under certain ondition, SHP undergoes a chemical reaction with the hydroxyl groups, resulting in crosslinking between CNCs.

The combination of the three crosslinkers described above can form crosslinked networks with high flexibility and good water stability. The resulting multiple crosslinked networks can wrap around the surface of the CNC chains and interact with their surface functional groups, subsequently disrupting the original hydrogen bond interactions between CNCs. This disruption can increase the water resistance of the composite.

1.4 Transparent Conductive CNC Films

Optoelectronic devices, including liquid crystal displays, light-emitting diodes, solar cells, touch panel displays, lasers, and detectors, play crucial roles across numerous domains and are indispensable in our daily lives. Their market size has been substantial and continues to expand steadily. An optoelectronic device requires at least one transparent electrode in order to emit or harvest light. Although indium tin oxide (ITO) currently dominates as the preferred material for transparent electrodes in optoelectronic devices, it has problems of scarce indium on earth which has caused the skyrocketing price, high mechanical brittleness that makes it unsuitable for flexible electronic devices. Consequently, there is an urgent need for the development of new transparent conductive materials to supplant ITO.[27] An idea of converting transparent CNC into conducting nanocomposite, which can combine the good optical property of CNC with conductive fillers is given in this thesis.

1.4.1 CNC as Templates for Conductive Films

CNC can be taken as a template to combine with other polymers boasting exceptional characteristics, to create functional polymer-based nanocomposites. It is suitable for the assembly of nanoparticles with characteristics such as anisotropy, birefringence, and liquid crystallinity, CNC has shown important applications in optical and electronic materials. [24]

So far CNC was mainly used as a dispersant for functional material or constituent for separator membranes or substrates for the preparation of conductive nanocomposite because of its insulator behavior.[15] However, it has several advantages of being the template of conductive nanocomposites. The nanosized CNC with a high aspect ratio can lower the percolation threshold via the formation of electrical networks with reduced functional material loading; The abundance of reactive surface hydroxyl groups on CNC facilitates simple chemical modification to obtain the desired electrical properties; The strong mechanical properties enable self-standing and high strength materials to be fabricated without additional additives; The high carbon content of CNC and its nanosized dimensions makes it an ideal precursor to

prepare porous carbon-based electrodes via a high-temperature pyrolysis; The high stability in aqueous suspension allow the water-based processes, which facilitates the use of environmentally friendly processes of production. Additionally, at high concentrations, CNC can self-assemble into a chiral-nematic crystalline phase.[23]

1.4.2 Flexible Conductive Films

With the increasing need of foldable display panels, touch screens, e-skin as well as implantable electronic devices, flexible transparent conductive films are essential components in realizing the design and development of flexible electronics.[26] The optoelectronic properties of different applications have specific requirements, for example, touch panels necessitate slightly flexible transparent conductive electrodes with high transmittance and relatively higher sheet resistance due to inductive functionality. Hence, there is a need for advanced materials, methodologies, and designs to cater to the needs of flexible electronics.[22]
Flexible conductive films can be made from a variety of inorganic, organic materials. Among inorganic materials, metals such as silver, gold, copper, and other hybrid materials have been used as flexible electrode materials due to their high electrical conductivity and flexibility. Besides ITO, metal oxides such as SnO_2, ZnO, In_2O_3, TiO_2, etc. have been widely used as transparent flexible electrodes due to their high transparency and conductivity. Carbon-based materials, like graphene, graphene oxide (GO), and carbon nanotubes(CNTs), are the first choice for flexible electrodes due to their high mechanical strength, flexibility, and excellent electrical conductivity. Organic polymers such as polypyrrole (PPy), poly(3,4-ethyl dioxythiophene) (PEDOT), and polyaniline (PANI) are also used as flexible electrodes due to their high conductivity and flexibility.[22]
Due to the inherent trade-offs between electrical conductivity and optical transparency as well as flexibility, It is hard to find a single material perfectly suitable for the flexible conductive films' fabrication. Therefore, the novel hybrid materials combined with different properties are created for fabricating advanced flexible conductive films to have improved transmittance, conductivity, and flexibility.[32]

1.4.2.1 Conductive Organic Polymers

Conductive organic polymers (COPs) are a good choice for making transparent conductive CNC composites, which can endow the composites with flexibility and conductivity. COPs are flexible, lightweight, and corrosion-resistant compared to inorganic conductive materials, and possess excellent electrical and optoelectrical properties, as well as photovoltaic capabilities. Another advantage of COPs is that their properties can be easily tuned through doping or post-treatment, allowing the materials to be tailored to meet the desired performance for a given application. Most of the electrical properties of conductive polymers originate from their conjugated pi-electron backbone. Representative examples such as polypyrrole (PPy), poly(3,4-ethyl dioxythiophene) (PEDOT), and polyaniline (PANI) have been extensively studied in recent years.[19]

Polypyrrole (PPy), as one of the most important azaheterocycles, due to its wide range of applications in pharmaceuticals and optoelectronic materials, coupled with its utility as an intermediate in natural products. Pyrrole itself is not naturally existed, but it occurs in many bioactive natural products. It was first found in nature by Runge in 1934, when he first noticed the formation of a new substance during the destructive distillation of coal tar and bone oil, which turned red upon application to acid-moistened pine splinters. Pyrrole and its derivatives have been the focus of attraction of material scientists because of their potential as components of optoelectronic materials such as polymeric light-emitting diodes (PLED) and organic light-emitting diodes (OLED), thin film transistors, non-linear optical polymers, high performance semiconductors derived from hexa(N-pyrrolyl)benzene.[18][20]The idea of forming transparent conducting films of Pyrrole: CNC and PEDOT: CNC films is given in this thesis with several attempts.

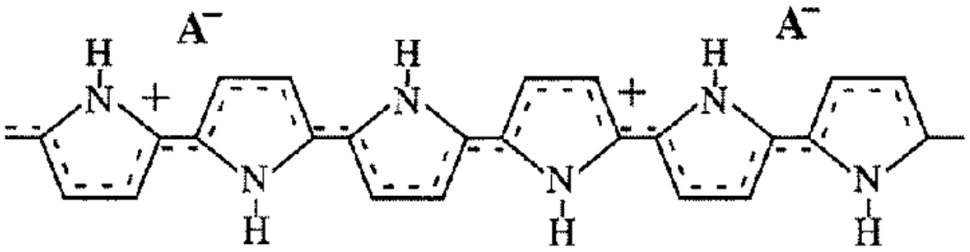

Figure 1.4: Chemical structures of polypyrrole

PEDOT is another popular conductive polymer that is derived from the monomer 3,4-ethylenedioxythiophene (EDOT). It is renowned for its high electrical conductivity, excellent stability and remarkable transparency, making it a versatile material for applications in electronics, optoelectronics, energy storage, and biomedical engineering. One of the distinguishing features of PEDOT is its flexibility, which allows for the fabrication of flexible and stretchable electronic devices. Furthermore, PEDOT can be easily doped with various dopants to further enhance its conductivity or modify its properties for specific applications. This tunability through doping enables precise control over PEDOT's electrical, mechanical, and optical characteristics, making it highly adaptable to diverse technological requirements. Poly(3,4-ethylenedioxythiophene):poly(styrenesulfonic acid) (PEDOT: PSS) is one of the most successful commercialized conducting polymer that meet different application requirements in organic electronics. [26] The specific conductivity of blue Aqueous PEDOT:PSS (CLEVIOS‘Ď‘ć PH 1000) dispersion is 850 S/cm and the Sheet Resistance Range is 100 - 1000 Ohm/sq. PEDOT: PSS possesses outstanding advantages of good film-forming properties, high transparency in the visible range, excellent thermal stability, especially the tunable and improved conductivity achieved by secondary doping.[30][27] The idea of forming transparent conducting PEDOT:CNC films is given in this thesis with several attempts.

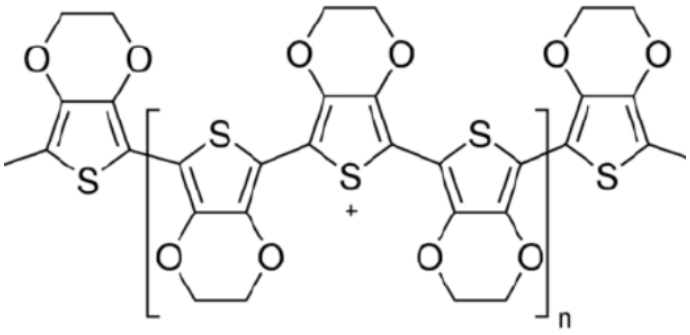

Figure 1.5: Chemical structures of PEDOT

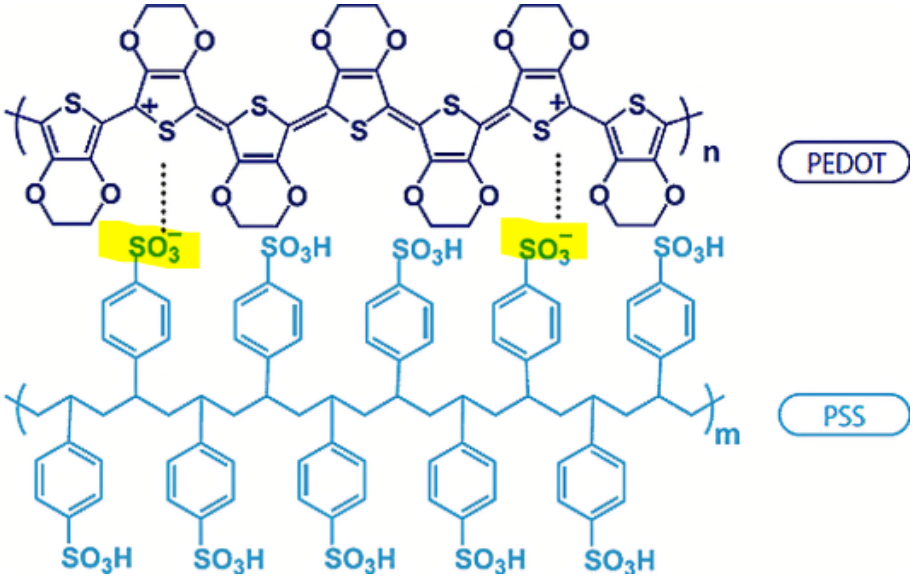

Figure 1.6: Chemical structures of PEDOT: PSS

1.4.3 Approaches for preparing Conductive CNC Composites

Conductive polymer and CNC hybrid materials have been widely studied due to its easy preparation method, low-cost, and various strategies to control the properties of the composite. There are mainly four categories of approaches for preparing the conductive CNC composites, which include conductive polymer coating, conductive metal coating, carbonized CNC and CNC-CNT composite. To obtain the transparent conductive CNC films and keep CNC's transparent optical properties, conductive polymer coating method is first considered to fabricate the conductive CNC composites.

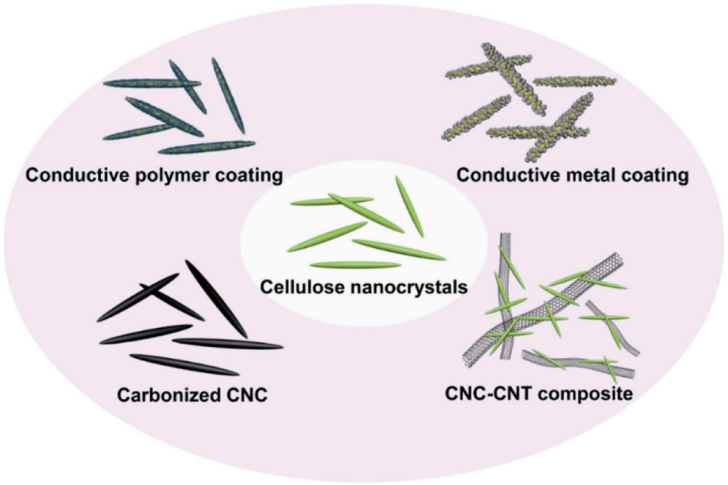

Figure 1.7: Schematic illustration describing the generalized approaches to prepare electrically conductive CNC

There are many studies dedicated to the fabrication of conductive polymer composites, where the conductive polymer and substrate material are used as the matrix.[2] The methods of combining conductive polymers and CNC can be divided into in-situ and ex-situ methods, depending on the presence of CNC during the polymerization.

For in-situ methods, conductive polymers are polymerized in the presence of CNC to form a core-shell structure, where the conductive polymer is coated on the CNC. The three typical polymerization techniques to fabricate conductive polymeric coating on CNC are chemical, photochemical, and electrochemical polymerizations. Chemical polymerization is the most commonly used technique to prepare core-shell conductive polymer coated CNCs because the process is scalable.[**?**] Another less popular method is electrochemical polymerization, the requirement of an electrochemical cell limited its development for synthesis. In ex-situ method, the conductive polymer and CNC are separately prepared. Usually, the conductive polymer is adhered to the CNC surface with physical mixing and blending method. This method is usually applied to lower the electrical percolation threshold and enhance the mechanical properties by bonding the conductive polymer with CNC network.[35]
Because of the conflicting properties of conductivity and transparency, one approach is to control the polymerization speed.

1.5 Characterization Techniques

1.5.1 ATR-FTIR

Fourier transform infrared (FTIR) spectroscopy is a form of vibrational spectroscopy for acquiring emission spectra or infrared absorption from solid, liquid or gas samples. This technique is based on the identification of functional groups within molecules where such groups stretching or bending when irradiated with specific wavelengths of light. These vibrations and their intensity (% transmission) are plotted against the frequency of the light (cm^{-1}) to which the sample is exposed to pro-

duce an FTIR spec4trum. The unique portion to the compound of the FTIR spectrum is called the fingerprint region. [9] Attenuated Total Reflection Fourier transform infrared (ATR-FTIR) spectroscopy is a label-free, non-destructive technique that can be applied to determine the organic content of the samples. Among the current techniques such as mass spectrometry (MS) and nuclear magnetic resonance (NMR), which can be expensive to run and have stringent sample pre-requisites for optimum results, which include but not limited to a pH range of 4-7, the use of a deuterated solvent, and the absence of excipients. The flexible, water-stable, transparent CNC films prepared in this thesis require minimal sample preparation and have not been tested under different pH levels and solvents. Therefore, FTIR was chosen as the characterization method, which can provide insights into sample components and be used to optimize the production process.[34]

When a molecule absorbs infrared radiation, its chemical bonds vibrate. The bonds can stretch, contract, and bend. This is why infrared spectroscopy is a type of vibrational spectroscopy. Fortunately, the complex vibrational motion of a molecule can be broken down into a number of constituent vibrations called normal modes. Molecules, like guitar strings, vibrate at specfic frequencies so different molecules vibrate at different frequencies because their structures are different. This is why molecules can be distinguished using infrared spectroscopy. The first necessary condition for a molecule to absorb infrared light is that the molecule must have a vibration during which the change in dipole moment with respect to distance is non-zero. The second necessary condition for infrared absorbance is that the energy of the light impinging on a molecule must equal a vibrational energy level difference within the molecule. If the energy of a photon does not meet the criterion in this equation, it will be transmitted by the sample and if the photon energy satisfies this equation, that photon will be absorbed by the molecule.

1.5.2 Sheet Resistance Measurement

1.5.2.1 Four-point Probe Method

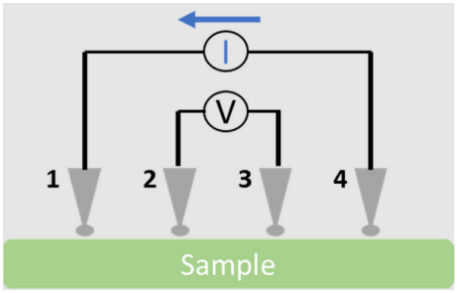

Figure 1.8: Schematic illustration of the four-point probe method

Sheet resistance (R_s), a critical electrical property, is used to characterize films of semiconducting and conducting materials. It is a measure of lateral resistance per square area of a film with uniform thickness, and quantifies the ability of electrical charge to travel in the plane of the film. The standard technique for measuring

sheet resistance is the four-point probe method. To calculate the R_s, a DC current is applied through the outer probes which includes a voltage across the two probes. By measuring this voltage drop, the sheet resistance can be calculated using the following Equation [26]:

$$R_s = \frac{\pi}{\ln(2)} \frac{\Delta V}{I} = 4.53236 \frac{\Delta V}{I} \tag{1.1}$$

Where:

$$\begin{aligned} R_s &= \text{Sheet Resistance (expressed in 'Ď'ę/sq.)} \\ \Delta V &= \text{Voltage drop measured across the inner probes} \\ I &= \text{Current applied at the outer probes} \end{aligned}$$

In addition to the factor $\frac{\pi}{ln(2)}$ in the equation above, a geometric correction factor is required, which accounts for the limitation of current pathways through the sample and this factor is based on the sample size, shape and thickness and the position of the probes. If the thickness of the material being measured is known, the sheet resistance can be used to calculate its resistivity by using the Equation [26] :

$$R_s = \frac{\rho}{t} \tag{1.2}$$

Where:

$$\begin{aligned} R_s &= \text{Sheet Resistance} \\ \rho &= \text{Bulk Resistivity} \\ t &= \text{Thickness of the Sample} \end{aligned}$$

The unit of the sheet resistance is $\Omega \cdot \mathrm{m}$, which is more completely stated in units of $\Omega \cdot \mathrm{m}^2/\mathrm{m}$ ($\Omega \cdot$ area/length), When divided by the sheet thickness (m), the units are Ω·m·(m/m)/m, the term " (m/m)" cancels, but represents a special "square" situation yielding an answer in ohms. An alternative, common unit is "ohms square" (denoted "$\Omega/\square$") or "ohms per square" (denoted "Ω/sq"), which is dimensionally equal to an ohm, but is exclusively used for sheet resistance. [13]

1.5.3 Polarized Optical Microscopy

Polarized Optical Microscopy, also referred to as Polarized Light Transmission Microscopy is a technique widely used to study the microstructure of crystals, liquid crystals, polymers, and other transparent, optically anisotropic specimens. A microscope image is the intensity distribution of the projection, on a viewing plane, of a light beam transmitted through a specimen. Polarized Optical Microscopy is a contrast-enhancing technique. Spatial variation in the intensity is called contrast. Contrast in most images arises because light is absorbed in different amounts as it traverses different parts of the specimen. However, contrast in images produced by polarized light microscopes also arises from variations in the phase change of light traversing the specimen. [5]

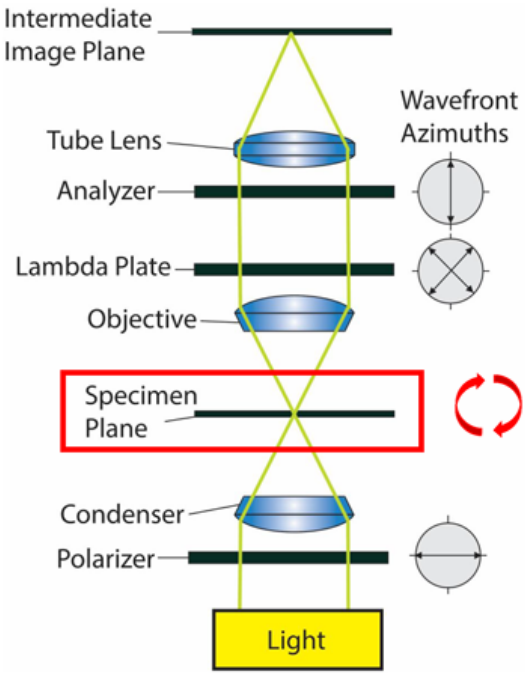

Figure 1.9: Scheme of a polarized light microscopy [31]

Light waves from the microscope lamp have randomly oriented planes of electric field oscillation, which also be called planes of polarization. The only light in which the electric field oscillates in parallel to the so-called privileged direction of the polarizer can pass through and be called plane-polarized light. When the privileged direction of the analyzer is oriented at right to that of the polarizer (i.e. they are at 90‘řC to each other), the field of view is in cross-polarized light, and the background will be dark. Image contrast arises from the interaction of plane-polarized light with a birefringent or doubly-refracting specimen to produce two individual wave components that are each polarized in mutually perpendicular planes. The velocities of these components, which are termed the ordinary and the extraordinary wavefronts, are different and vary with the propagation direction through the specimen. After transmitting the specimen, the light components become out of phase, but are recombined with constructive and destructive interference when they pass through the analyzer. [31]

The polarized light microscope allows observing samples that are visible primarily due to their optically anisotropic character. Anisotropic materials have optical properties that vary with the orientation of the incident light with respect to the crystallographic axis. Such materials have more than one refractive index (for example, azurite, cinnabar, etc.) and with such microscopes will appear bright and distinctly coloured against the black background. However, these are polarization colours (not actual sample colours) and are related to the refractive indices and thickness of the sample. In cross-polarized light, isotropic materials (e.g. gasses, liquids, resins, unstressed glasses, cubic crystals that have only one refractive index) will not be visible. [31]

2

Materials and Equipment

Materials

Chemical Name	Producer
Sulfate Cellulose Nanocrystals Solution	Jelka Feldhusen
Triethanolamin	ALDRICH (98%)
Ethylene glycol diglycidyl ether	ALDRICH (50%)
Methanol	ALDRICH (99.9%)
Sodium hypophosphite	Flucka (98%-100%)
1,2,3,4-Butanetetra-carboxylic acid	ALDRICH (99%)
Potassium persulfate	SIGMA-ALDRICH (99%)
3,4-Ethylenedioxythiophene	SIGMA-ALDRICH (97%)
Pyrrole	ALDRICH (98%)
Iron(III) chloride	SIGMA-ALDRICH (97%)

Note: Sulfate Cellulose Nanocrystals solution was produced by Jelka Feldhusen, the hydrolysis of microcrystalline cellulose by using 64 wt% sulphuric acid from Avicel.

Equipment

Equipment Name	Producer
Sonicator	SONICS
Titration Device	Titrando 905
Molecularporous Membrane Tubing	Spectra/Por
Petri dish	Gosselin 100 x 15 mm Petri Dishes
Source measure unit	Keithley
Optical Goniometer	Attension
FT-IR Spectrometer	Perkin Elmer
Optical Microscope	ZEISS
Pipette	VWR
Balance	Sartorius
Fridge	Ninolux

3

Methods and Experiments

3.1 Dialysis

Dialysis is a separation technique used to separate molecules or particles based on differences in their sizes or properties, such as molecular weight or charge. It is commonly employed to purify and concentrate solutions of macro-molecules. There are three components of Dialysis setup, sample chamber, dialysis chamber and semi-permeable membrane. Due to the differences in concentration and electrochemical gradients, molecules or ions can pass through the membrane via diffusion.

During the thesis work, 1 wt% SCNC solution was dialyzed, and deionized water was taken as the buffer solution. The basic principle of this passive transport procedure involves osmosis and diffusion. Due to the ion concentration inside the membrane is higher than that of the outside, water molecules keep moving into the dialysis tube to balance out and maintain the homeostasis at equilibrium through the hypotonic progress. At the same time, small molecules sulfuric acid in the SCNC solution keep moving out of the membrane.

Based on the molecular size of SCNC and hydrogen sulfate ions, MWCO 12-14 KD dialysis membranes (Standard RC Tubing) were chosen for this experiment, that means the dialysis membrane has a molecular weight cut-off in the range of 12,000 to 14,000 daltons. Small molecules with a molecular weight (size) below this range will pass through the pores of the membrane, while larger molecules SCNC with a molecular weight above this range will be effectively retained and not able to diffuse through the membrane. The experiments are performed in the following steps: Pull 1 liter of 1 wt% SCNC solution into deionized-water-moistened membrane, tied both ends tight. Conductivity of deionized water was checked with hours interval and plotted into diagrams. The dialysis progress was stopped when water conductivity was less than 5 μS.

3.2 Sonication

Sonication is a technology applying sound energy to agitate particles. In this thesis situation, sonication is carried out to disperse the SCNC and make crosslinker and SCNC combined with each other. Sonication is performed in plastic containers and amplitude 40% applied, the probe is immersed into the sample solution. Long-time sonication may overheat the solution and cause the sulphate groups on the surface of the SCNC hydrolyses. The sulphate groups are not only the reactive fuctional groups but also provide the electrostatic stabilization to the suspension system. CNC aggregations and clumps will be formed if the sulfate groups are hydrolyzed.

3.3 Titration

Titration, also known as titrimetry and volumetric analysis, is a method of quantitative chemical analysis to determine the concentration of an identified analyte. A reagent, termed the titrant or titrator, is prepared as a standard solution of known concentration and volume. The titrant reacts with a solution of analyte, which may also be termed the titrand, to determine the analyte‘ts concentration. The volume of titrant that reacted with the analyte is termed the titration volume.

In this thesis work, potentiometric titration was used to determine the number of sulfate half ester content of CNC, they are titrated and determined by 0.1 M NaOH solution under room temperature with stirring. The protons on the sulphate groups remaining from the synthesis will be neutralised by the hydroxyl ions. The pH and conductivity of the CNC solution were measured and plotted with a function of time and volume of NaOH added. The conductivity of suspension will reach two peaks in consequence.

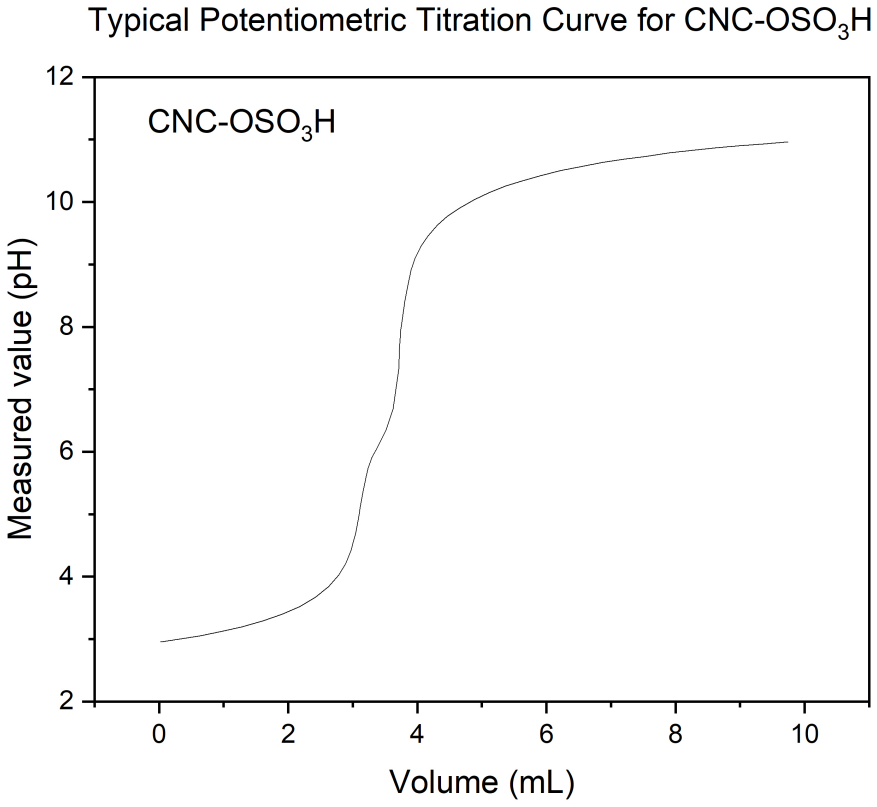

Figure 3.1: Scheme of typical potentiometric titration curve for SCNC

0.5 wt% SCNC solution was used as the analyte, prepared from the dialyzed 1 wt% SCNC solution diluted from a 3.85 wt% batch. The solutions were all prepared with milli-Q water and stored in a refrigerator (0°–5°). Three samples with 25 ml SCNC and 40 μL 0.5 M NaCl added were prepared in plastic containers for titration, while the remaining SCNC solution was collected for dry weight determination.

Before starting the titration, each sample was sonicated 30s for reducing the CNC aggregation. The titration was done in triplicates, so that standard deviation can calculated. After starting the Tiamo 3.0 software and calibration, the system was ready to go and select 'CNC sulphate pH to 11, NaOH 0.01 M' as the method to perform the titration. Once the titration was complete, the electrodes were removed, rinsed and placed back in appropriate storage solution.

3.3.1 Dry weight determination

The SCNC dry weight determination was performed in the following steps. First, took three cleaned diameter approximate 50mm watch glass, and placed into 50° oven for 24 hours, then measured the dry watch glass weights by 4 decimals. After adding several drops of SCNC (0.5-1.0 g), the mass of watch glass was weighted again. The watch glasses were put into the 50° oven for 24 hours for dring after adding the sample, the mass of watch glass after drying was again be weighted, each weighting process was repeated for three times to get the average value.

3.4 Film Fabrication

The entire film fabrication procedure can be divided into two stages. The first stage involves creating the water-stable CNC films. The second stage focuses on producing conductive water-stable CNC films while attempting to maintain transparency. The second stage is still under exploration, and the most promising formulations and methods are described in the following sections.

3.4.1 Flexible Water-stable CNC Films Preperation

The water-stable CNC films are prepared in the following steps with the illustration. First, prepare a 1 wt% sulfated CNC solution by diluting from the stock solution. Prepare 100 $\mu mol/mL$ water solutions of Triethanolamine (TEOA), 1,2,3,4-Butanetetracarboxylic acid (BTCA), Sodium hypophosphite (SHP), and Ethylene glycol diglycidyl ether (EGDE) separately. Then, add TEOA into the solution with a 1:1 molar ratio of the sulfate groups on CNC and sonicate the mixture for 30 seconds for conjugation. Next, add the BTCA, SHP, and EGDE solutions sequentially, followed by another 30 seconds of sonication to thoroughly mix the solution. Finally, pour the solution into a petri dish and allow it to dry on the bench. All operations up to this point were conducted at room temperature. After approximately 2 days of drying, the film was peeled off, put on the glass watch glass and placed into an oven heated to 140‘řC for 30 minutes. Then, a small piece of the film was cut and placed into a 50 mL plastic bottle filled with 30 mL deionized water, ethanol, acetone, methanol, isopropanol for 24 hours to test its stability.

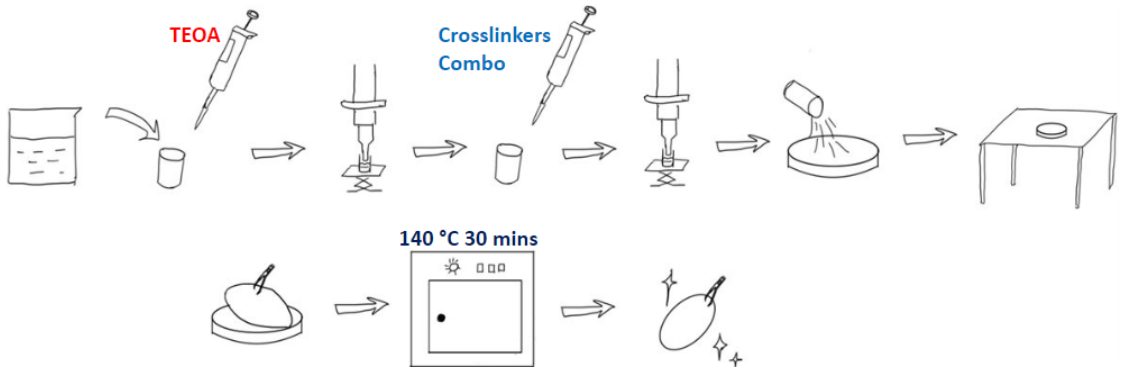

Figure 3.2: Scheme of Transparent water-stable CNC films preparation

To create a flexible transparent water-stable film with a thickness of approximately 20 μm and an area of 63.62 cm^2, the formulation is shown in the table below.

Sulfate groups amount of CNC	TEOA	BTCA	SHP	EGDE
$30\mu mol$	$30\mu mol$	$30\mu mol$	$60\mu mol$	$15\mu mol$

Table 3.1: Flexible transparent water-stable film formulation

3.4.2 Flexible Water-stable Transparent Conductive CNC Films Preperation

There are two categories of methods that have been tried for making the conductive CNC films: in-situ and ex-situ methods, as described in the introduction. For in-situ method, pyrrole monomers are polymerized in the CNC solution, while for ex-situ method, the CNC films are immersed in the pyrrole monomers solution. The most conductive transparent water-stable CNC film was fabricated by using the ex-situ method with pyrrole.

3.4.2.1 Ex-situ Polymerization Method

Two solutions for the later polymerization progress were prepared: the oxidants solution and the pyrrole monomer solution. The oxidants 4.485×10^{-3} mol potassium persulfate (PPS) and 5.995×10^{-3} mol iron(III) chloride ($FeCl_3$) were dissolved in the 100 mL mixture of methanol and deionized water with a volume ratio of 1:9. while a 1 mmol/mL pyrrole solution dissolved in Methanol.

The specific steps for making the films are as follows: First, prepare a flexible water-stable CNC film as described in the last subsection. Then add the oxidants solution into a diameter 90mm petri dish and immerse the film into it. Put the petri dish into the fridge for 1 hour and then take it out, slowly dropping the prepared pyrrole solution into the petri dish. Put it back into the fridge for another 4 hours, then wash it with ethanol and deionized water, and let it dry on the bench at room temperature for 24 hours.

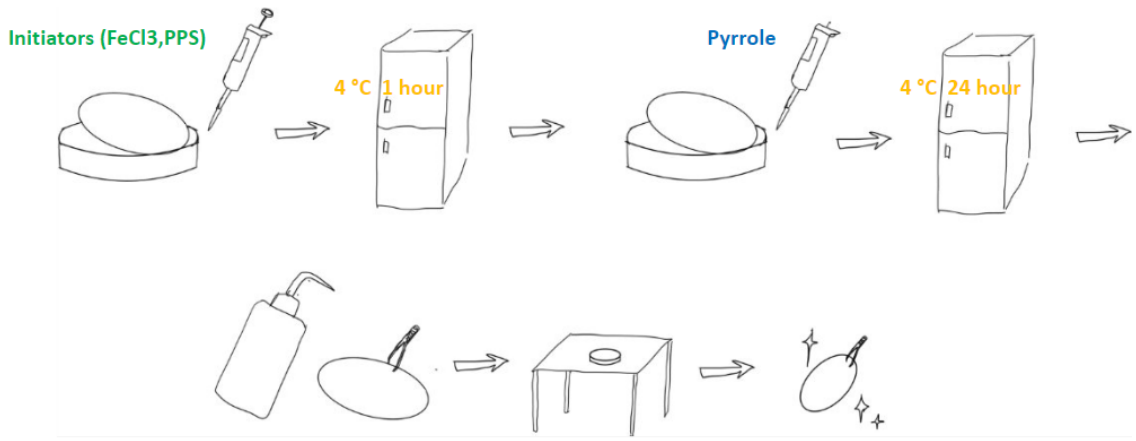

Figure 3.3: Scheme of the Ex-situ method of preparing the conductive transparent water stable CNC films

To create the most conductive transparent water-stable CNC film among all with a thickness of approximately 20 μm and an area of 16 cm^2 (1/4 area of the diam. 90 mm petri dish), the formulation is shown in the table below.

Sulfate groups amount of CNC (μmol)	TEOA (μmol)	BTCA (μmol)	SHP (μmol)	EGDE (μmol)	Pyrrole (μmol)	$FeCl_3$ (μmol)	PPS (μmol)
30	30	30	60	15	1000	239.8	179.4

Table 3.2: Conductive water-stable film formulation (Ex-situ Method)

3.4.2.2 In-situ Polymerization Method

Limited concentration of pyrrole can be added to the system via the in-situ method during this thesis work. The maximum molar ratio of sulfate groups on CNC to pyrrole was 1:5 among all the ex-situ experimental groups. Beyond this ratio, the CNC/Pyrrole film sticks to the bottom of the petri dish or it is black and opaque. Therefore, the method for preparing the transparent CNC/Pyrrole film with the highest amount of pyrrole added is presented as followed.

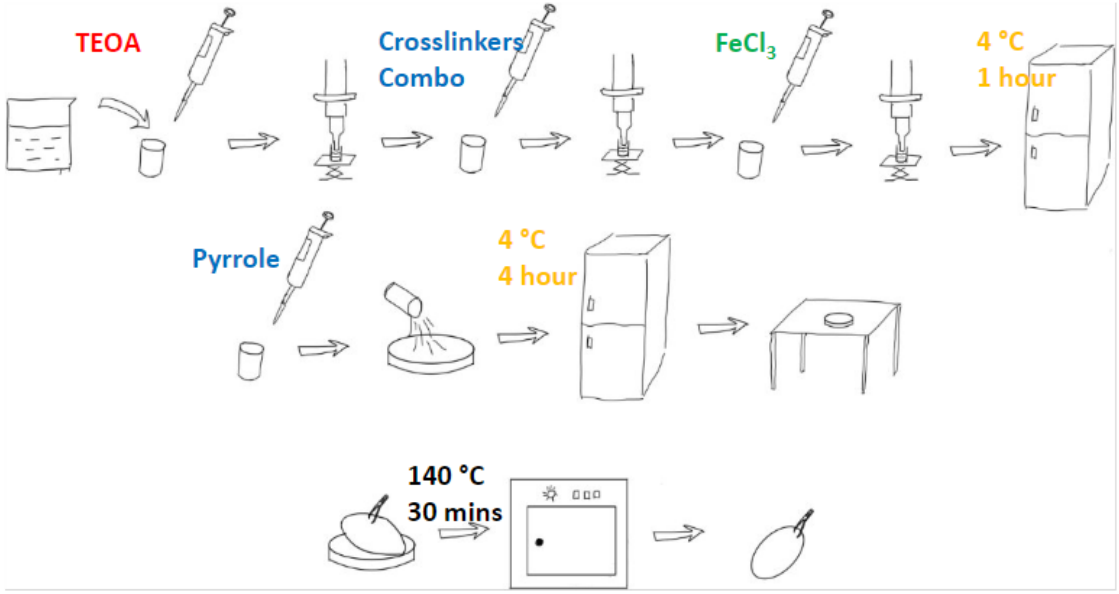

Figure 3.4: Scheme of the In-situ method of preparing the conductive transparent water stable CNC films

First is to prepare all the solutions that are needed for the reactions. 1 wt% CNC solution, 1 mmol/mL pyrrole MeOH solution, 10 $\mu mol/mL$ $FeCl_3$ water solution, solution and 100 $\mu mol/mL$ water solutions of TEOA, BTCA, SHP, and EGDE are prepared separately. Then add Triethanolamine (TEOA) into the solution with a 1:1 molar ratio of sulfate groups on CNC and sonicate the mixture for 30 seconds. Next, add the same molar ratio of Sodium hypophosphite (SHP), 1,2,3,4-Butanetetra-carboxylic acid (BTCA), and two times molar ratio of Ethylene glycol diglycidyl ether (EGDE) solutions sequentially, followed by another 30 seconds of sonication after all the crosslinkers were added to thoroughly mix the solution. Follow with adding the pre-cooled $FeCl_3$ solution into the mixture and slowly add drops of the pyrrole solution, pour the mixture into a petri dish then place it into the fridge with a lid on for 4 hours. Finally, take it away from the fridge and remove the lid, then let it dry on the bench at room temperature for two days to form the film.

Sulfate groups amount of CNC (μmol)	TEOA (μmol)	BTCA (μmol)	SHP (μmol)	EGDE (μmol)	$FeCl_3$ (μmol)	Pyrrole (μmol)
30	30	30	60	15	5	150

Table 3.3: Flexible water-stable with pyrrole added film formulation (In-situ Method)

3.5 Characterization

3.5.1 Polarized Optical Microscopy

All the films were observed by Optical Microscope (ZEISS) with "Transmitted light (Polarized)" mode. The polarizing microscope is equipped with both a polarizer, positioned in the light path somewhere before the film sample, and an analyzer (a second polarizer),

placed in the optical pathway between the objective rear aperture and the observation tubes or camera port. The scheme of the polarized light microscopy is shown below. Image contrast arises from the interaction of plane-polarized light with a birefringent (or doubly-refracting) specimen to produce two individual wave components that are each polarized in mutually perpendicular planes. The velocities of these components are different and vary with the propagation direction through the specimen. After exiting the specimen, the light components become out of phase, but are recombined with constructive and destructive interference when they pass through the analyzer.[31]

3.5.2 ATR-FTIR Spectroscopy

To characterize the components of the sample, ATR-FTIR techniques are chosen for the experiments. ATR-FTIR has largely surpassed transmission and is now the primary measurement technique used as this method involves minimal sample preparation and is non-destructive. To use ATR-FTIR, the sample is simply placed on top of a crystal which is typically made of diamond, germanium, or zinc selenide. The IR light is directed through the crystal where it is partially absorbed by the sample. The IR light then passes through the crystal again and is detected.[8] The scheme of FTIR spectroscopy is shown below. The model used for all the film samples analysis is Spectrum Two (Serial no - 100300) in 400 to 4000 cm-1 wavenumber range. After setting up the model and calibration, a small piece of film was cut and were subjected to FTIR analysis with a resolution of 4 cm-1 and 30 FTIR scans. The existing functional groups in the film samples were then be confirmed by investigations.

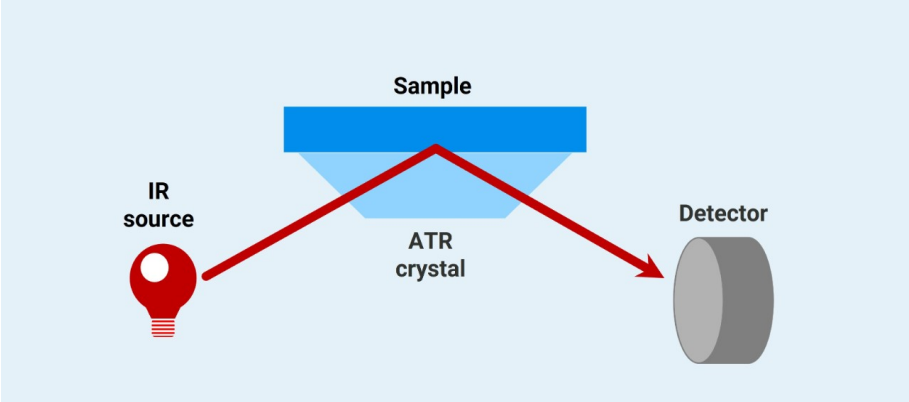

Figure 3.5: Scheme of FT-IR Spectroscopy[8]

3.5.3 Four Point Probe Method

The "four-point probe" (4PP) method is the most common and simplest technique for measuring the sheet resistance (Rs) of the thin films. The equipment shown in the picture has four equally spaced, co-linear probes which are used to make electrical contact with the material to be characterized. A source measurement unit (SMU) together with the four-point probe setup was used to measure the sheet resistance of all the samples. After the sample was placed in the holder and the probes were put in contact with the film, the target current was applied via the SMU and the voltage drop was subsequently measured.[26] The controlling and visualizing software was created by Youngseok Kim. During the test, the applied current unit and range were adjusted according to the plots of the data until

all the dots exhibited a linear relationship. Each film was tested three times in different places, and the average sheet resistance was recorded. After testing the sheet resistance, the thickness of the films was measured using a digital micrometer gauge with a resolution of 0.001 mm. The thickness of each film was measured three times, and the average value was calculated.

4

Results

4.1 Titration

The sulfate half ester content of each CNC sample was determined though a potentiometric titration. By adding NaOH, the pH titration went from 3.4 to 10.1. The scheme of the reaction during the titration is shown in the figure. [17][36]

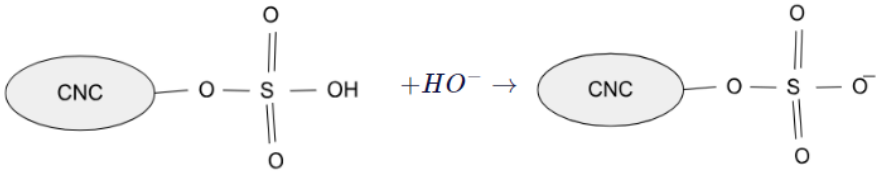

Figure 4.1: Scheme of half-ester sulfate groups and the hydroxyl groups during titration

The dry substance content is the percentage of solids in a mixture of substances. The higher this proportion, the drier the mixture. The unit of DS content is [% by weight], and the formula for calculating the dry substance content of a suspension is shown below.[10]:

$$\text{DS content [\% by weight]} = \left(\frac{\frac{\rho(\text{liquid})}{\rho(\text{suspension})} - 1}{\frac{\rho(\text{liquid})}{\rho(\text{solid})} - 1} \right) * 100$$

Figure 4.2: Formula for calculating the dry substance content of a suspension

Where:

$$\rho(liquid) = \text{density of the pure liquid}$$
$$\rho(Solid) = \text{density of the pure solid}$$
$$\rho(Suspension) = \text{density of the suspension}$$
$$D_Scontent = \text{Dry substance content}$$

Based on the maximum ERC (endpoint recognition criteria) level, the equivalence point was determined where the first peak appeared. The volume Veq corresponds to equivalence point used to calculate the sulfate content by following equation[25]:

$$Sulfatecontent(mmol/g) = \frac{C \times V_{eq}}{M_s \times D_m} \times 100 \tag{4.1}$$

Where:

$$\begin{aligned} C &= \text{Concentration of the NaOH} \\ V_{eq} &= \text{Volume of NaOH} \\ M_s &= \text{Total suspension weight} \\ D_m &= \text{Suspension concentration} \end{aligned}$$

The long storage time of CNC may have caused the half-ester sulfate groups on the surface to interact between molecules, potentially affecting the accuracy of the sulfate group quantification. Therefore, two times of dialysis (23-10-23 and 24-01-18) and four times of titration including dry weight content determination were performed over the four months of film fabrication. The calculation results of the sulfate content and dry weight determination are shown in the below table according to the equation.

The results of the dry weight determination on 23-11-03 and 24-01-18 were not accurate because the mass of the watch glass after adding the substrate was not measured timely by the balance. Waiting too long for a stable reading caused excessive water evaporation, resulting in a reading smaller than the actual value. Consequently, the dry weight concentration is smaller and $-OSO_3^-$ concentration appear larger than they truly are.

Date	0.5 wt%	1 wt%	$-OSO_3^-$ Concentration ($\mu mol/g$)
23-10-23	0.65	–	260.5
23-11-03	0.45	0.97	320.8
24-01-18	0.31	–	406.5
24-02-05	0.54	0.92	195.5

Table 4.1: Titration and Dry Weight Determination Results

4.2 Films Observation and Characterization

In this section, flexible transparent water-stable films and flexible transparent conductive water-stable films prepared by in-situ and ex-situ methods along with the characterization results are presented. The challenges faced during the attempts are also analyzed.

4.2.1 Flexible Transparent Water-stable CNC Films

The pure sulfated CNC films are fragile and show cracks after drying. With TEOA added into the solution, the dispersion of CNC particles is enhanced and the matric mobility is increased, which results in a more homogeneous film with enhanced flexibility. Besides, contains hydroxyl groups (-OH) that can form hydrogen bonds with the hydroxyl groups present on the surface of CNC particles. These hydrogen bonds can increase the intermolecular interactions between TEOA and CNC, resulting in a more flexible and cohesive film structure.

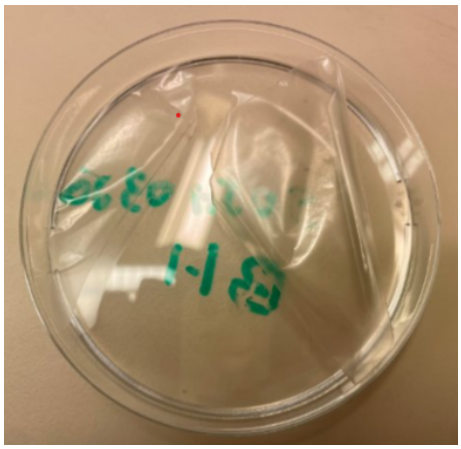

Figure 4.3: A flexible transparent water-stable CNC film

Furthermore, to enhance the water resistance of the flexible CNC films, several different types of crosslinkers have been tried to improve hydrophobicity. Together with TEOA, BTCA, EGDE, and SHP are added to make the film water stable. The pure sulfated CNC films and the sulfated CNC films with only TEOA added are easily dissolved in water, because the forces between crystallites are very weak. After placing the films into water, the water molecules diffuse into the crystallite network and disperse the CNC. BTCA, EGDE, and SHP are three kinds of crosslinkers that have suitable lengths to link the crystals. N,N,N',N'-Tetramethyl-1,4-diaminobutane (NNNN), and Poly(ethylene glycol) diglycidyl ether (PEG) had also been tried, while the short linkers may result in stiffness of the films, whereas a long linker with 25 or more atoms, such as PEG, may make the film swell and turn into a gel after adding water. The experimental results show that the molar ratio of sulfate groups on CNC: TEOA: BTCA: SHP: EGDE is 1:1:1:2:0.5 for the additives combination that can produce the flexible and water-resistant film. Except for deionized water, the film also showed good stability in ethanol, acetone, methanol, and isopropanol after 24 hours of immersion in the solvent. After taking the film out of the solvent and drying it again, the flexibility of the film remained.

Figure 4.4: The Picture of Pure CNC film cracked into two pieces

The Polarized Optical Microscopy pictures had been taken. From the left to right, they are the pure CNC Film, TEOA, BTCA, EGDE, and SHP (molar ratio 1:1:2:0.5) CNC film, and TEOA, BTCA, EGDE, and SHP (molar ratio 1:1:2:5) CNC film. With the additives added into the system, the microscopy picture of the film showed more even and smooth texture than the pure CNC film, while the film with high concentration of the crosslinkers had star-shape crystal structure precipitate out.

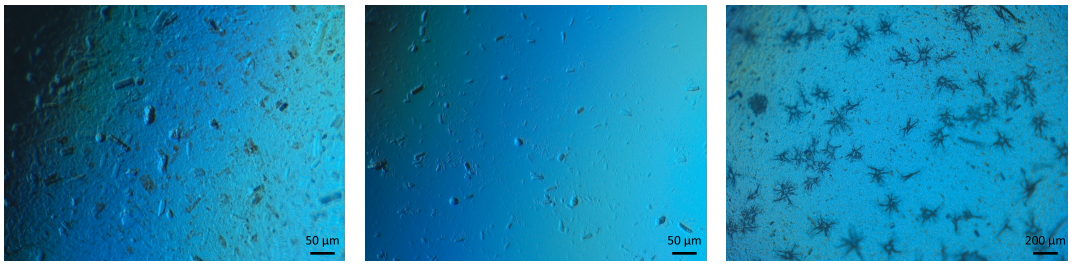

Figure 4.5: POM pictures of CNC films

4.2.2 Flexible Water-stable Transparent Conductive CNC Films

The observations of the conductive films are grouped into two parts: ex-situ and in-situ preparation methods. The conductivity of the films is tested using the four-point probe method, and the ATR-FTIR spectroscopy analysis results are presented for the in-situ method prepared CNC/PPy film.

4.2.2.1 In-situ Polymerized Film

For the films formed using the in-situ polymerization method, the monomers of conductive polymers (EDOT or Pyrrole) are added to the CNC water suspension. PPS and $FeCl_3$ are used to initiate the polymerization of the monomers to form conductive polymer-coated CNC. Many factors, such as the concentration of the oxidant, solvent, reaction temperature, CNC/monomer molar ratio, and oxidant/monomer molar ratio, affect the polymerization and properties of the films, ultimately determining their performance.

For the CNC/PPy, molar ratios of 1:1, 1:5, 1:15, and 1:50 of CNC half-ester sulfate groups and pyrrole were tried. However, only films prepared with molar ratios of 1:1 and 1:5 could be peeled off from the petri dish. Therefore, a molar ratio of 1:5 was selected as the optimum concentration for further work in this thesis. $FeCl_3$ and pyrrole with a molar ratio of 1:50 were used to initiate the PPy polymerization after attempting higher ratios of 1:10, 1:2, and 1:1. After adding 1:1 and 1:2 of $FeCl_3$ into the CNC and Pyrrole monomers mixture, it formed into a gel where $FeCl_3$ drops were located. Although a higher concentration of $FeCl_3$ can theoretically improve the conductivity of the film due to the nature of ions, the transparency of the films is affected, as shown in the picture below.

Figure 4.6: CNC/PPy pictures with 1:1 molar ratio of $FeCl_3$ and Pyrrole

To control the polymerization speed of the pyrrole, low-temperature (4‘řC) reaction conditions were applied. After heating the film in an oven at 140‘řC for 30 minutes to activate the crosslinkers, the film became more fragile and brittle. The color of the film was light brown before heating and turned to grey after heating. The picture of the CNC/PPy film prepared with the formulation listed in the method part (before heating) is presented below. It forms into a completely transparent film, while the color of the edge part is darker than the central. After heating the film and testing its water resistance as well as resistance to other solvents, it showed good stability in ethanol, acetone, methanol, and isopropanol after 24 hours of immersion in the solvent.

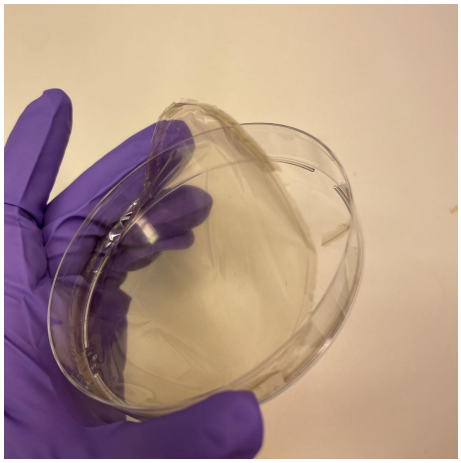

Figure 4.7: CNC/PPy film with the 3.4.2.2 formulation (Before heating)

To characterize the components of the film, ATR-FTIR spectroscopy was used to identify the key chemical bonds of CNC, Pyrrole, EGDE, and SHP. The overall spectra are shown below to compare the differences between films with SHP and EGDE added. Batch-1, Batch-6, and Batch-10 contain EGDE, while Batch-1, Batch-4, and Batch-9 contain SHP.

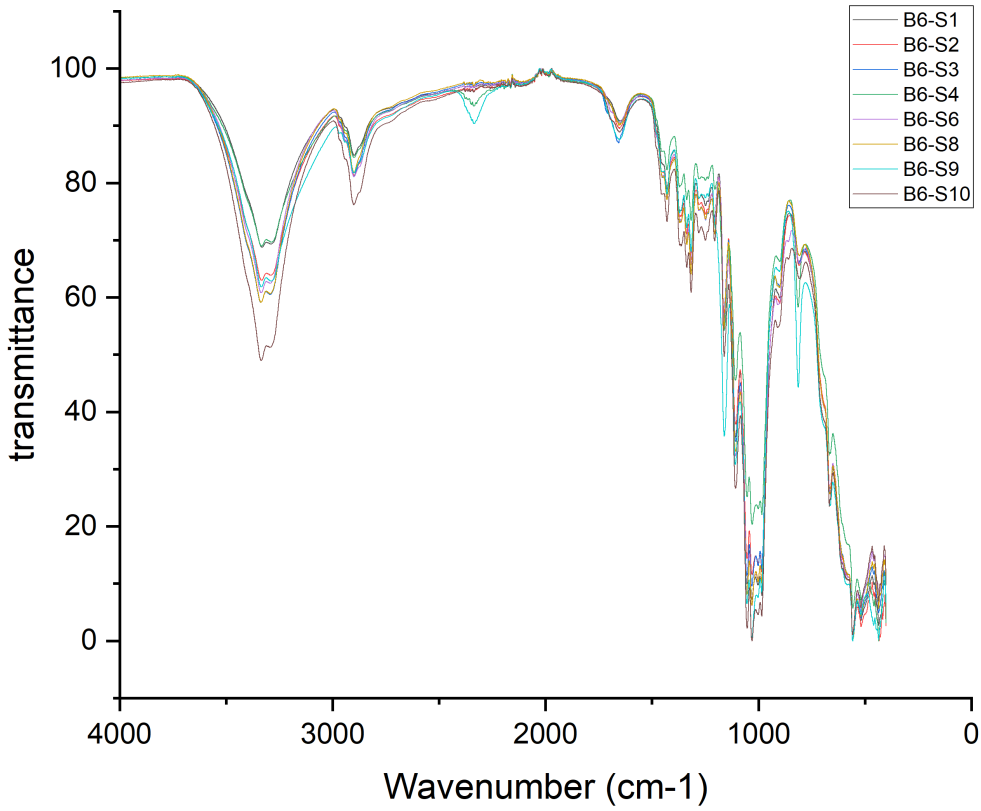

Figure 4.8: ATR-FTIR spectra for CNC/PPy with different crosslinkers.(overview)

The Batch-6 FTIR spectrum was selected for SHP and Batch-4 for EGDE analysis. In Batch-6, the SHP-added spectrum, the peak at the wavenumber 3338 cm^{-1} indicates the hydroxyl group in CNC, the band centered at 2900 cm^{-1} is attributed to asymmetric and symmetric stretching vibrations of aliphatic C-H bonds in CNC. Additionally, the band located at 1053 cm^{-1} is related to the C-O-C pyranose ring vibration. Peaks at 2333 cm^{-1} and 812 cm^{-1} may indicate the presence of SHP [33]. Furthermore, the detected peaks at 1446 cm^{-1} indicate the symmetric stretching vibration for the C=N bond of Pyrrole, and the shown peaks at 1023 cm^{-1} are representative of the existing H-C= vibration bond in polypyrrole, while the 1156 cm^{-1} and 905 cm^{-1} may represent for the doping state of PPy In the ATR-FTIR spectra for the Batch-9 sample with EGDE added, similar peaks of CNC and pyrrole are observed, and the wide peaks 1694 cm^{-1} and 1652 cm^{-1} may represent for EGDE.

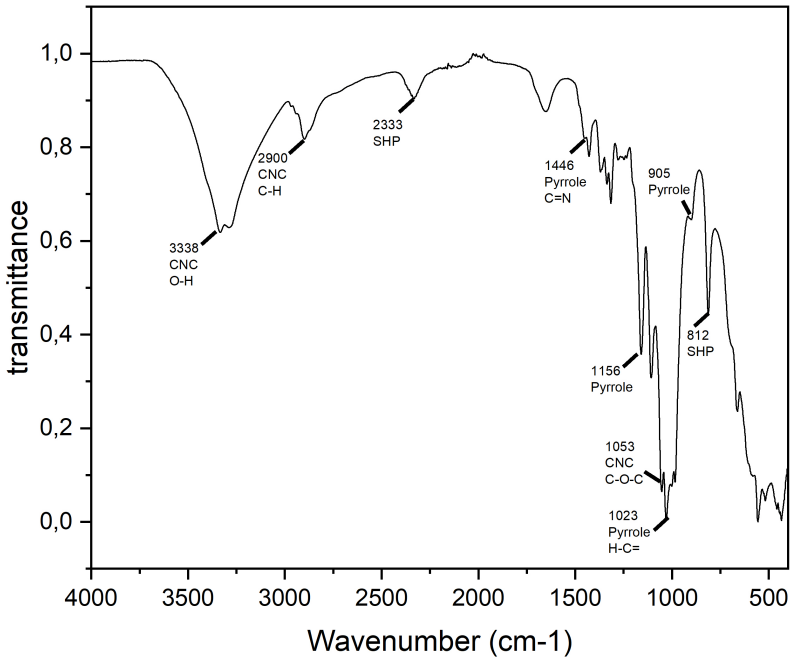

Figure 4.9: ATR-FTIR spectra for CNC/PPy with SHP

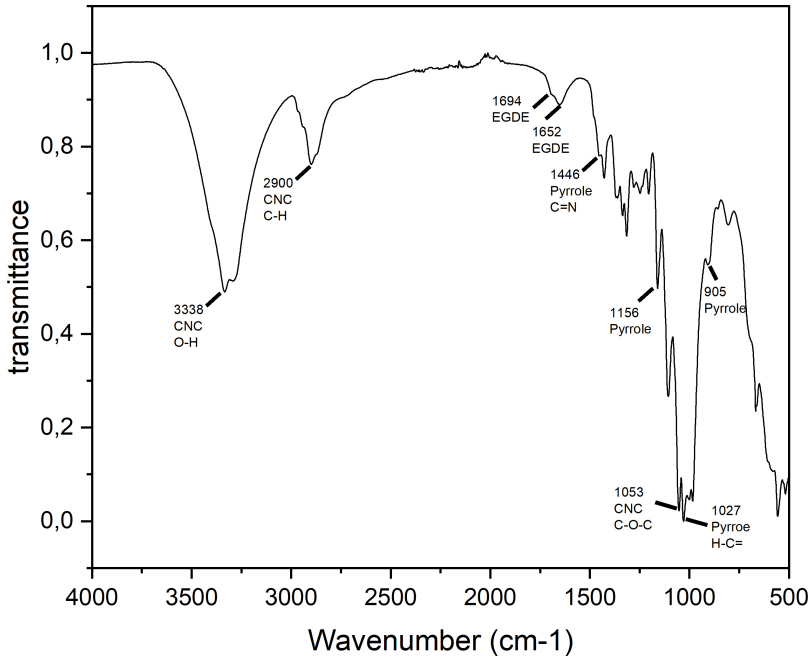

Figure 4.10: ATR-FTIR spectra for CNC/PPy with EGDE

Figure 4.11: Pictures of flexible conductive CNC films with different concentrations of pyrrole and oxidants

Though the formulation described in the method had the highest ratio of Pyrrole added into the system, the conductivity of the film could not be detected by the four-point probe method. When applying the minimum current on the top, the voltage did not show a linear relationship with the applied current, indicating that the result was out of range. The Electrochemical Impedance Spectroscopy (EIS) method was also tried for in-situ PPy/CNC films, but it yielded a similar result of being out of range. In this situation, an improved method for increasing the conductivity of the film is needed, thus the ex-situ method was proposed.

4.2.2.2 Ex-situ Polymerized Film

To solve the problem of films can not be peeled and the limited amount of pyrrole added into the system by using the in-situ polymerization method, the ex-situ polymerization method was coming up. which is to fabricate the transparent water-stable CNC film first, then immerse it in the oxidants and monomer solution to polymerize.

The most conductive transparent CNC film was produced by the ex-situ method, with the formulation described in section 3.4.2.1.(left picture of 4.10) The sheet resistance was tested using the four-point probe method, and the thickness was measured using a digital micrometer gauge. The calculated result using equations 1.1 and 1.2 is 2.2×10^8 ohm/sq. If the concentrations of Pyrrole and the oxidants are 4 times higher, the film becomes opaque and black (right picture of 4.10), with a sheet resistance of 2.6×10^6 ohm/sq. The pictures of the two films are shown above.

4.2.3 Challenges

4.2.3.1 Oxidant choices

It is expected that the films prepared using $FeCl_3$ have stronger mechanical strength and better conductivity because of the synergy of iron(III) ion chelation and the hydrogen bonds (H-bonds) between the OH groups of CNC, and amino groups of PPy chains. [12] Besides using $FeCl_3$ as the initiator of PEDOT/CNC mixture, ferrous sulfate heptahydrate had also been tested, though the results all showed the samples cannot be peeled from

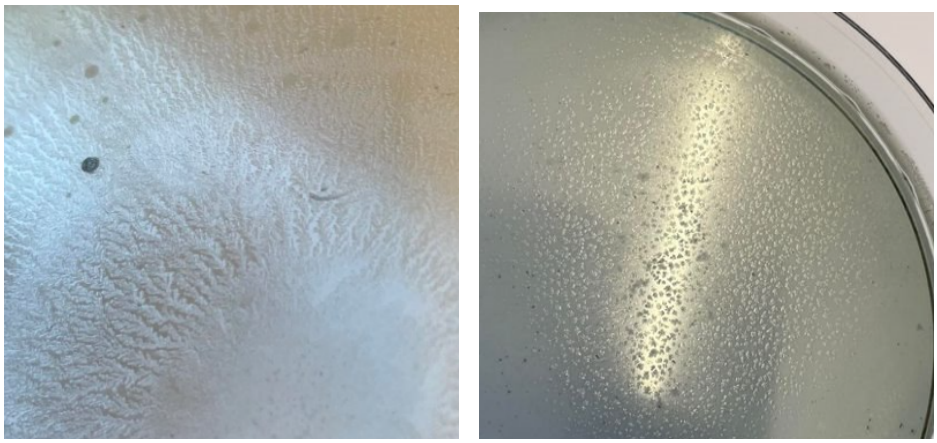

Figure 4.12: Pictures of $FeCl_3$ added PEDOT/CNC film (left) with ferrous sulfate heptahydrate added PEDOT/CNC film (right)

the petri dish, the $FeCl_3$ added groups showed more transparent and smooth surface than the Ferrous sulfate heptahydrate added group. The coffee ring effect showed in ferrous sulfate heptahydrate added group may indicate the polymerization rate is high, that may because the Ferrous ions start to oxidize, creating sulfate radicals from persulfate, and it starts to aggregate very fast, forming a denser material that starts to absorb all the solution around it.[14] The mixture with $FeCl_3$ showed centralized ramification structure and the ferrous sulfate heptahydrate added mixture showed darker color and star-like cluster structure on the surface, that may because the Ferrous sulfate heptahydrate yields more sulfate radicals than $FeCl_3$.

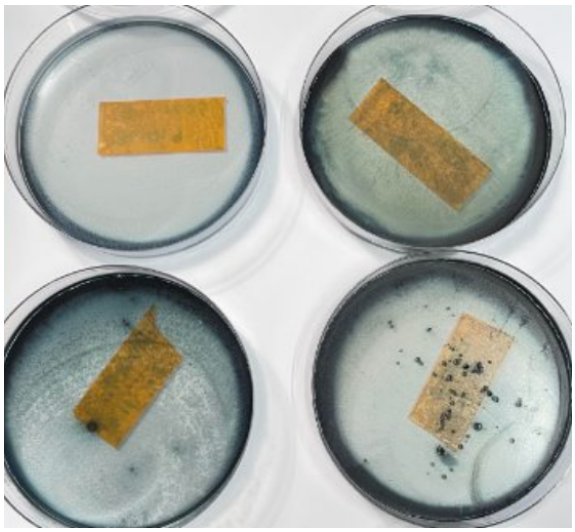

Figure 4.13: The coffee ring effect showed in CNC/PEDOT samples

4.2.3.2 In-situ method with PEDOT

Using EDOT as the monomer for CNC/PEDOT film making has also been tried with the in-situ method, while phase separation during the mixing step was very obvious. EDOT monomers (liquid) were immiscible in water. Though EDOT monomers can be dissolved in ethanol, after mixing with the CNC water solution, they separated again. The prob-

lem can be slightly improved by sonification, but after pouring the mixture of EDOT and CNC into the petri dish and waiting for several hours, the EDOT floated on the surface as dots. After water evaporation, the mixture stuck to the bottom of the petri dish (both glass and polystyrene have been tried), and it was hazy and showed a grey color.

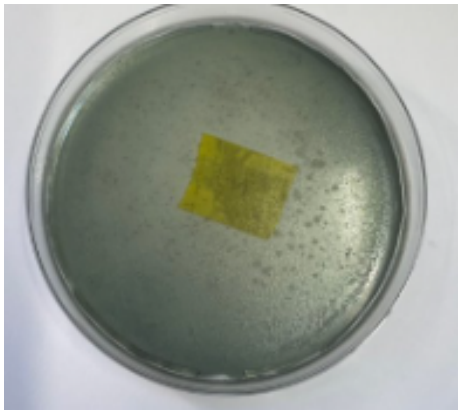

Figure 4.14: PEDOT/CNC sample by using in-situ method

4.2.3.3 Surface modification of CNC

Favorable surface chemistry of the CNC is necessary to promote the interaction between the functional groups on its surface (hydroxyl, carboxylic, or sulfuric) and conductive polymer (NH_2 on PPy, heterocyclic sulfur on PEDOT). To improve that films stuck at the petri dish problem and improve the hydrophobic property of the films, the surface modification of CNC with Azetidinium salts had been tried. 1 wt% CNC was modified with two different azetidinium salts, namely C6-C6-N-Azet-Cl (1,1-diallyl-3-hydroxyazetidin-1-ium) and All-All-N-Azet-Cl (1,1-dihexyl-3-hydroxyazetidin-1-ium) respectively.

The ratio of the azetidinium salts to SCNC dispersion was taken in accordance of a 1:1.1 molar ratio of sulfate content: Azetidinium salt. Conjunction of Azetidinium salt to sulfate half ester was done by heating the mixture at 90° for 4 hours. After the reaction, the mixture was cooled down to room temprature. In order to remove the unreacted azetidinium reagent, the reaction mixture was in 12-14 kD MWCO dialysis tubing and dialyzed by deionized water for 48 hours. Conductivity was measured approximately every 12 hours, and the dialysis procedure was done until the conductivity was below 5 ‘ţS, then the solutions were transferred into plastic bottles.

After the conjunction of azetidinium salt, Az-CNC suspensions (C6-C6-N-Azet-CNC and All-All-N-Azet-CNC) were used to replace the SCNC in the formulation of 3.4.2.2, while keeping the oxidant $FeCl_3$ and pyrrole ratio unchanged. However, neither the C6-C6-N-Azet-Cl modified CNC/PPy films nor the All-All-N-Azet-Cl modified CNC/PPy films met expectations, they are even more sticky compared with the SCNC group. The control groups are Az-CNC + TEOA, Az-CNC + TEOA + BTCA + SHP + EGDE, Az-CNC + TEOA + Pyrrole + $FeCl_3$. But still the C6-C6-N-Azet-Cl modified group failed to form any films, while the All-All-N-Azet-Cl modified group only produced thin and fragile films in the PS petri dish with TEOA added, these films could not be peeled off when the crosslinker combinations and pyrrole were added. Compared with the SCNC+TEOA groups, the films were thinner, more fragile, and could not be peeled off as whole films.

The reason for these failed attempts may be due to inappropriate synthesis operations. Additionally, no characterization was applied to the modified CNC suspensions, so the results cannot be fully trusted.

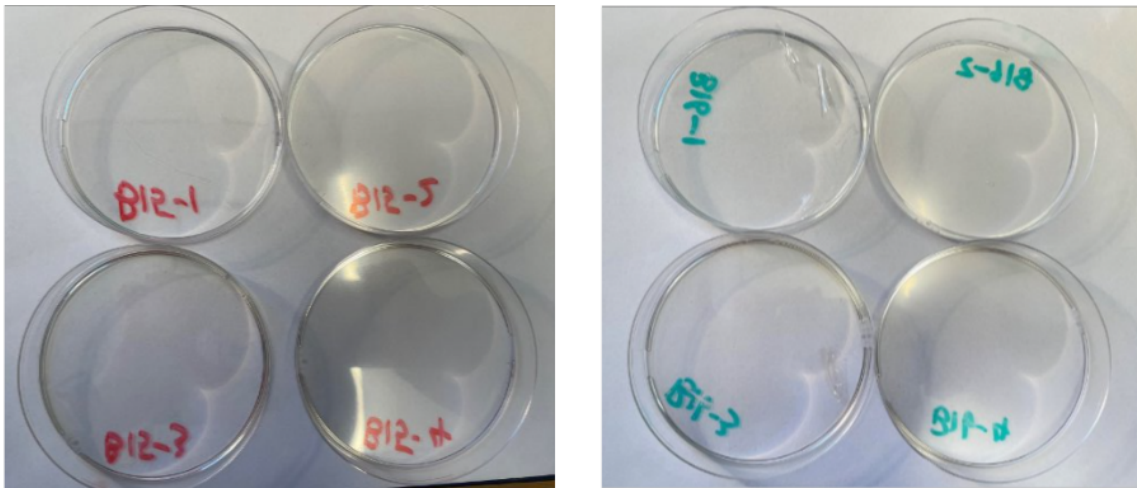

Figure 4.15: Pictures of C6-C6-N-Azet-Cl-CNC (left) and All-All-N-Azet-Cl-CNC films (right)

4.2.3.4 Transparency limitation

When the $FeCl_3$ and pyrrole with a 1:1 molar ratio were mixed together, aggregation occurred very quickly, resulting in black precipitation separating out from the suspension. This affected the color and haze level of the film. Processing the samples under 4‘řC to control the polymerization rate resulted in limited improvement; although the time until the color turned dark was prolonged, it eventually still turned black and hazy. If transparency is desired and pyrrole is to be used, other polymerization methods might be worth trying, such as photopolymerization. Additionally, other conductive organic polymers such as polyaniline (PANI) and colorless oxidants are worth exploring in future work.

4.2.3.5 Conductivity limitation

The conductivity was improved by using the ex-situ film-making method compared with the in-situ method, but the sheet resistance was still relatively high. The commercial PEDOT:PSS (CLEVIOS‘Ď‘ć PH 1000) dispersion sheet resistance is 100 - 1000 Ohm/sq, which means the conductivity 1×10^5 - 1×10^6 times higher than the flexible transparent conductive CNC/PPy films and 1×10^3 - 1×10^5 times higher than the most conductive black opaque CNC/PPy film prepared in this thesis work. Though the presence of iron(III) ions can greatly contribute to the electrical conductivity, the yellow-green color greatly affected the transparency of the films. Thus only a very small amount of iron(III) ions was added in the formulation and its contribution to the conductivity can be neglected.
The Electrochemical Impedance Spectroscopy (EIS) method was also attempted for in-situ PPy/CNC films, but the signal was out of range. The main reason is that the conductivity of the films is too low to be detected, and another reason may be that the tested sample was not processed appropriately. Considering the project's goal of making the film as conductive as possible, no further tests were performed using the EIS method.

5
Conclusion

The investigation into the fabrication of flexible transparent conductive films using sulfated cellulose nanocrystals (CNC) and the conductive organic polymer pyrrole has been studied through a series of characterization involving titration, film observation, polarized optical microscopy, ATR-FTIR spectroscopy, and sheet resistance measurement. The challenges faced during attempts for future work have also been provided.

Firstly, the determination of sulfate half-ester content in CNC suspension revealed variations due to factors such as storage time and dry weight content accuracy. In the fabrication of flexible transparent water-stable CNC films, the addition of tetraethylenediamine (TEOA) and crosslinkers combination of benzoyl peroxide (BTCA), ethylene glycol diglycidyl ether (EGDE), and styrene hydroperoxide (SHP) proved instrumental in enhancing film flexibility and water resistance, polarized optical microscopy images revealed the film structure and texture of the film.

Several challenges have been faced in the synthesis of flexible water-stable conductive films using in-situ polymerization methods. While attempts with polypyrrole (PPy) showed the result that is more in line with expectations, issues such as the inability to peel off the film and the limited amount of pyrrole monomers that can be added into the system were encountered. The use of azetidinium-salt-modified CNC suspensions to replace the SCNC, EDOT monomers to replace the pyrrole monomers and different oxidants have been tried to improve the performance of the films but did not fully address the transparency and conductivity limitations.

In exploring alternative methods, the ex-situ polymerization method was proposed to enhance conductivity. By immersing pre-formed water-resistant CNC films in oxidant and monomer solutions, films with improved conductivity were achieved. Nevertheless, challenges such as opaque films and fragility after oxidation remain for further investigation.

Overall, the research highlights the flexible transparent water-stable cellulose nanocrystals film fabrication method. In-situ and ex-situ polymerization methods with conductive organic polymers Pyrrole and PEDOT; various oxidants and processing conditions were explored, demonstrating that ex-situ fabrication is a promising method for preparing the flexible transparent water-stable conductive CNC film. Future research could explore additional types of conductive organic polymers and polymerization methods to enhance the conductivity of the films while balancing the trade-off with transparency. Further innovations are essential to unlock the full potential of CNC-based films in flexible optoelectronics, sensors, and energy devices.

Bibliography

[1] Muhammad Mustafa Abeer, Mohd Cairul Iqbal Mohd Amin, and Claire Martin. A review of bacterial cellulose-based drug delivery systems: their biochemistry, current approaches and future prospects. *Journal of Pharmacy and Pharmacology*, 66(8):1047–1061, 8 2014.

[2] Faris M. Al-Oqla, S. M. Sapuan, T. Anwer, M. Jawaid, and M. E. Hoque. Natural fiber reinforced conductive polymer composites as functional materials: A review, 2015.

[3] Mehran Alavi. Modifications of microcrystalline cellulose (MCC), nanofibrillated cellulose (NFC), and nanocrystalline cellulose (NCC) for antimicrobial and wound healing applications, 2019.

[4] Huiyu Bai, Shuhao Hu, Haiyan Zhu, Shengwen Zhang, Wei Wang, and Weifu Dong. Constructing a cellulose based chiral liquid crystal film with high flexibility, water resistance, and optical property. *International Journal of Biological Macromolecules*, 250:126132, 10 2023.

[5] J R Bellare, H T Davis, W G Miller, and L E Scriven. Polarized optical microscopy of anisotropic media: Imaging theory and simulation. *Journal of Colloid and Interface Science*, 136(2):305–326, 1990.

[6] Mikaela Börjesson, Karin Sahlin, Diana Bernin, and Gunnar Westman. Increased thermal stability of nanocellulose composites by functionalization of the sulfate groups on cellulose nanocrystals with azetidinium ions. *Journal of Applied Polymer Science*, 135(10), 2018.

[7] L Brinchi, F Cotana, E Fortunati, and J M Kenny. Production of nanocrystalline cellulose from lignocellulosic biomass: Technology and applications. *Carbohydrate Polymers*, 94(1):154–169, 2013.

[8] BRUKER. Measurement techniques in infrared spectroscopy, 2024.

[9] N N Daéid. FORENSIC SCIENCES | Systematic Drug Identification. In Paul Worsfold, Alan Townshend, and Colin Poole, editors, *Encyclopedia of Analytical Science (Second Edition)*, pages 471–480. Elsevier, Oxford, 2005.

[10] Flottweg SE. Dry substance content (DS content).

[11] I Golovtsov, S Bereznev, R Traksmaa, and A Öpik. Thin composite films consisting of polypyrrole and polyparaphenylene. *Thin Solid Films*, 515(19):7712–7715, 2007.

[12] Lian Han, Songbo Cui, Hou-Yong Yu, Meili Song, Haoyu Zhang, Nathan Grishkewich, Congguo Huang, Daesung Kim, and Kam Michael Chiu Tam. Self-Healable Conductive Nanocellulose Nanocomposites for Biocompatible Electronic Skin Sensor Systems. *ACS Applied Materials & Interfaces*, 11(47):44642–44651, 11 2019.

[13] Michael Heaney. Electrical Conductivity and Resistivity. pages 7–1. 1 2003.

[14] Sebasti‘ąn Hernández, Joseph K Papp, and Dibakar Bhattacharyya. Iron-Based Redox Polymerization of Acrylic Acid for Direct Synthesis of Hydrogel/Membranes and Metal Nanoparticles for Water Treatment. *Industrial & Engineering Chemistry Research*, 53(3):1130–1142, 1 2014.

[15] Fanny Hoeng, Aurore Denneulin, and Julien Bras. Use of nanocellulose in printed electronics: A review, 2016.

[16] Bingxue Hu, Hongbin Pu, and Da-Wen Sun. Multifunctional cellulose based substrates for SERS smart sensing: Principles, applications and emerging trends for food safety detection. *Trends in Food Science & Technology*, 110:304–320, 2021.

[17] Jelka Feldhusen. *Synthesis of Azetidinium Salts and their Applications on Nanocellulose*. PhD thesis, Chalmers University of Technology, Gothenburg, 2023.

[18] Jonas Jusélius and Dage Sundholm. The aromatic pathways of porphins, chlorins and bacteriochlorins. *Physical Chemistry Chemical Physics*, 2(10):2145–2151, 2000.

[19] Gagan Kaur, Raju Adhikari, Peter Cass, Mark Bown, and Pathiraja Gunatillake. Electrically conductive polymers and composites for biomedical applications, 2015.

[20] Rajni Khajuria, Sumita Dham, and Kamal K. Kapoor. Active methylenes in the synthesis of a pyrrole motif: An imperative structural unit of pharmaceuticals, natural products and optoelectronic materials. *RSC Advances*, 6(43), 2016.

[21] F Khelifa, Y Habibi, and P Dubois. Chapter 5 - Nanocellulose-Based Polymeric Blends for Coating Applications. In Debora Puglia, Elena Fortunati, and Jos‘ľ Maria Kenny, editors, *Multifunctional Polymeric Nanocomposites Based on Cellulosic Reinforcements*, pages 131–175. William Andrew Publishing, 2016.

[22] S Kumar and Y Seo. Flexible Transparent Conductive Electrodes: Unveiling Growth Mechanisms, Material Dimensions, Fabrication Methods, and Design Strategies. *SMALL METHODS*, 8(1), 2024.

[23] Yebin Lee, Haoyu Zhang, Hou-Yong Yu, and Kam C Tam. Electroconductive cellulose nanocrystals ‘Ă‘Ť Synthesis, properties and applications: A review. *Carbohydrate Polymers*, 289:119419, 2022.

[24] Ao Liu, Hailian Wu, Abid Naeem, Qing Du, Bin Ni, Hongning Liu, Zhe Li, and Liangshan Ming. Cellulose nanocrystalline from biomass wastes: An overview of extraction, functionalization and applications in drug delivery, 2023.

[25] Johannes Lützenkirchen, Tajana Preocanin, Davor Kovačević, Vladislav Tomišić, Lars Lövgren, and Nikola Kallay. Potentiometric Titrations as a Tool for Surface Charge Determination. *Croatica Chemica Acta*, 85:391–417, 12 2012.

[26] Mira Naftaly, Satyajit Das, John Gallop, Kewen Pan, Feras Alkhalil, Darshana Kariyapperuma, Sophie Constant, Catherine Ramsdale, and Ling Hao. Sheet resistance measurements of conductive thin films: A comparison of techniques. *Electronics (Switzerland)*, 10(8), 2021.

[27] Jianyong Ouyang. "secondary doping" methods to significantly enhance the conductivity of PEDOT:PSS for its application as transparent electrode of optoelectronic devices. *Displays*, 34(5), 2013.

[28] Tejal V Patil, Dinesh K Patel, Sayan Deb Dutta, Keya Ganguly, Tuhin Subhra Santra, and Ki-Taek Lim. Nanocellulose, a versatile platform: From the delivery of active molecules to tissue engineering applications. *Bioactive Materials*, 9:566–589, 2022.

[29] Abdus Salam, Lucian A. Lucia, and Hasan Jameel. A novel cellulose nanocrystals-based approach to improve the mechanical properties of recycled paper. *ACS Sustainable Chemistry and Engineering*, 1(12), 2013.

[30] Hui Shi, Congcong Liu, Qinglin Jiang, and Jingkun Xu. Effective Approaches to Improve the Electrical Conductivity of PEDOT:PSS: A Review. *Advanced Electronic Materials*, 1(4), 2015.

[31] Koit Herodes Signe Vahur, Ivo Leito. Polarized light microscopy.

[32] Jizhong Song, Jianhai Li, Jiayue Xu, and Haibo Zeng. Superstable transparent conductive Cu@Cu4Ni nanowire elastomer composites against oxidation, bending, stretching, and twisting for flexible and stretchable optoelectronics. *Nano Letters*, 14(11), 2014.

[33] Lucas Tonette Teixeira, Wanderson Ferreira Braz, Rog'lrio Navarro Correia de Siqueira, Omar Ginoble Pandoli, and Mauro Cesar Geraldes. Sulfated and carboxylated nanocellulose for Co+2 adsorption. *Journal of Materials Research and Technology*, 15:434–447, 2021.

[34] Hannah Tiernan, Bernadette Byrne, and Sergei G Kazarian. ATR-FTIR spectroscopy and spectroscopic imaging for the analysis of biopharmaceuticals. *Spectrochimica Acta Part A: Molecular and Biomolecular Spectroscopy*, 241:118636, 2020.

[35] Evgeniy Tkalya, Marcos Ghislandi, Wim Thielemans, Paul Van Der Schoot, Gijsbertus De With, and Cor Koning. Cellulose nanowhiskers templating in conductive polymer nanocomposites reduces electrical percolation threshold 5-fold. *ACS Macro Letters*, 2(2), 2013.

[36] Sylwia Wojno, Amit Kumar Sonker, Jelka Feldhusen, Gunnar Westman, and Roland Kádár. Isotropic Gels of Cellulose Nanocrystals Grafted with Dialkyl Groups: Influence of Surface Group Topology from Nonlinear Oscillatory Shear. *Langmuir*, 39(18):6433–6446, 5 2023.

[37] Hongli Yang, Jesper Edberg, Viktor Gueskine, Mikhail Vagin, Mehmet Girayhan Say, Johan Erlandsson, Lars Wågberg, Isak Engquist, and Magnus Berggren. The effect of crosslinking on ion transport in nanocellulose-based membranes. *Carbohydrate Polymers*, 278:118938, 2022.

DEPARTMENT OF SOME SUBJECT OR TECHNOLOGY
CHALMERS UNIVERSITY OF TECHNOLOGY
Gothenburg, Sweden
www.chalmers.se

CHALMERS
UNIVERSITY OF TECHNOLOGY